*Int. J. Electrochem. Sci.*, 16 **(2021)** Article Number: 211227, doi: 10.20964/2021.12.24

**International Journal of ELECTROCHEMICAL SCIENCE**
www.electrochemsci.org

# Synthesis and Application of Nanocomposite of ZnS, $Ni_2P$ and Reduced Graphene Oxide as Electrochemical Sensor for Determination of Chlorpyrifos in Farmland Water

*Wei Zheng*[1], *Jing Sui*[1,*], *Tiantian Chen*[2], *Qingxue Qi*[3], *Ying Lv*[1]

[1] Department of Metallurgy and Construction Engineering, Laiwu Vocational and Technical College, Jinan, 271100, China
[2] Department of Biotechnology Engineering, Taishan Vocational and Technical College, Taian, 271000, China
[3] Shandong Laiwu Xueye Lake National Wetland Park Management Office, Jinan, 271100, China
[*]E-mail: Suijjjj1@126.com

*Received:* 21 August 2021 / *Accepted:* 27 September 2021 / *Published:* 10 November 2021

This study was performed on the synthesis of ZnS, $Ni_2P$ and reduced graphene oxide (ZnS@$Ni_2P$/rGO) nanocomposite as an electrochemical sensor of chlorpyrifos (CPS) in farmland recirculated waters. The electrodeposition method was used to modify a glassy carbon electrode (GCE) surface with rGO, ZnS and $Ni_2P$ nanoparticles. Morphological and structural analyses using SEM and XRD showed that defects in rippled nanosheets of rGO on GCE provided the substrate for high porous and high crystalline electrodeposition of ZnS@$Ni_2P$ nanoparticles which led to a higher effective surface area and could effectively promote the electron transfer of the electrode. Results of electrochemical studies using DPV and amperomerty indicated sensitive, selective and stable responses of ZnS@$Ni_2P$/rGO/GCE to the presence of CPS. Results indicated a wide linear response range from 25 to 375 µM with a high sensitivity of 0.89799 µA/µM and a limit of detection of 0.004 µM. Comparison of the obtained sensing properties with the previously reported sensors illustrated the comparable electrochemical performance of ZnS@$Ni_2P$/rGO/GCE, which was correlated to the high electron transfer rate contributed by the edge-rich architecture of the rGO and catalysis sites of ZnS and $Ni_2P$ nanoparticles. The modified CPS sensor demonstrated good accuracy in prepared real samples of agricultural recirculated water, with appropriate recovery ($\geq$ 92.50%) and RSD ($\leq$3.31%) values. Therefore, ZnS@$Ni_2P$/rGO/GCE can be reliable for the determination of CPS in farmland recirculated water and agricultural wastewater samples.

**Keywords:** Chlorpyrifos; Nanocomposite; ZnS; $Ni_2P$; Reduced graphene oxide; Farmland waters; Amperomerty

## 1. INTRODUCTION

Chlorpyrifos (CPS, O,O-Diethyl O-(3,5,6-trichloropyridin-2-yl) phosphorothioate) is an organophosphate insecticide and pesticide that is used to control foliage and soil-borne insect pests [1, 2]. CPS insecticidal action is based on the inhibition of the enzyme cholinesterase which as a neurotransmitter regulates the neurotransmitter acetylcholine in the nervous system [3, 4]. Acetylcholine accumulates in the insect's nerve endings and between neurons, and by irreversibly inhibiting acetylcholinesterase, causes the formation of a stronger, longer-lasting signal to the next neuron which results in excessive transmission of nerve impulses, and the death of the target pest [5-7]. Moreover, it is reported that CPS can damage the human nervous system and it is considered moderately hazardous to humans by the World Health Organization based on its acute toxicity [8, 9].

CPS can produce a runny nose, tears, and excessive saliva or drooling in tiny quantities [10-12]. Sweating, headaches, nausea, and dizziness are all possible side effects. Acute intoxication with vomiting, abdominal muscular cramps, muscle twitching, tremors and weakness, and loss of coordination can result from more extreme exposures. Excessive exposure has been related to neurological consequences, long-term developmental problems, and immunological conditions [13-15]. Children's mental development may be harmed if exposure occurs during pregnancy. Furthermore, ingested CPS is drastically absorbed into the blood and leads to death.

Therefore, there are many laws and limitations regulating pesticide use by private, commercial, urban and agriculture, and many researchers have been conducted on FTIR [16], High-performance liquid chromatography [17], gas chromatography [18], liquid chromatography [19], mass spectrometry [20], chemiluminescence [21], UV Spectrophotometry [22], flame ionization detection [23] and electrochemical methods [24-28] for detection of CPS in vegetables, fruit and industrial and agriculture wastewaters. Among these methods, electrochemical methods can be considered as rapid and low-cost pesticides analyses [29]. Moreover, modification of electrode surface nanostructured materials can promote the selectivity and stability of sensors in sequential analyses. As a result, the synthesis of ZnS@$Ni_2P$/rGO/GCE as that of an electrochemical sensor for CPS in agricultural recirculated waters was investigated.

## 2. EXPERIMENT

### *2.1. Synthesis of nanocomposite*

The electrodeposition method was used for modification of the GCE surface with rGO, ZnS and $Ni_2P$ nanoparticles. Before the electrodeposition, the GCE surface was polished with an alumina slurry (99%,Dengfeng Hongsheng Abrasives Co., Ltd., China) and rinsed in ethanol (95%, Shijiazhuang Chemical Tech Co., Ltd., China) and DI water, respectively. The electro-position was conducted on an Autolab potentiostat/galvanostat (PGSTAT30, Eco Chemie, Utrecht, Netherlands) using a three-electrode cell which is contained Ag/AgCl (KCl 3M) as the reference electrode, the clean GCE as the working electrode and Pt plate as the counter electrode. The electrodeposition of rGO nanoparticles on GCE was performed in the electrolyte containing 1.0 mg/ml rGO (>99wt%, 1-5 μm, The Graphene Box, Spain) in 0.07M PBS pH 9 at potential range of -1.5 V to +0.5 V at scan rate of

10mV/s during 30 cycles [30]. Electrodeposition of ZnS nanoparticles on GCE was also performed in the electrolyte solution contained 0.1mM of $ZnSO_4.5H_2O$ (99, Sigma-Aldrich) and 1mM $Na_2S_2O_3$ (≥99%, Sigma-Aldrich) at potential of -1.3 V for 20 minutes [31, 32]. The electrodeposition of $Ni_2P$ nanoparticles on GCE was carried out in an electrolyte solution containing 0.15 M of $Ni(NO_3)_2$ (99.9%, Sigma-Aldrich) and 0.15M $NaPO_2H_2$ (≥99%, Sigma-Aldrich) at a potential of -1.0 V for 10 minutes [33]. For simultaneous electrodeposition of ZnS and $Ni_2P$ nanoparticles on GCE or rGO/GCE, the electrolyte solution containing 0.1mM of $ZnSO_4.5H_2O$, 1mM $Na_2S_2O_3$ as ZnS sources, and 0.15 M of $Ni(NO_3)_2$ and 0.15M $NaPO_2H_2$ as $Ni_2P$ sources in an equal volume ratio was prepared, and electrochemical deposition was conducted at potential range of -1.4 V to -0.5 V at scan rate of 10mV/s during 50 cycles.

### *2.2. Characterization*

Differential pulse voltammetry (DPV) and amperometry measurements were carried out using the Autolab electrochemical system in an electrochemical cell which is contained Pt plate, and Ag/AgCl (KCl 3M) and bare or modified GCE as working electrodes. The electrolyte for electrochemical measurements was 0.05 M tetrabutylammonium bromide (TBAB, ≥99.0%, Sigma-Aldrich) containing ethanol solution in a volume ratio of 6:4. Scanning electron microscopy (SEM, JEOL, JSM-6010LV, USA) was applied for morphological studies of modified GCE, and X-ray diffraction (XRD, D/max-2200 vpc, Rigaku Corporation, Japan) was used for analyses the structure of the electrodeposited nanocomposite on GCE.

### *2.3. Real samples preparation*

For preparation of the real sample, CPS (20% (v/v)) was purchased from the local market. 1ml of CPS (contained 0.2ml of CPS) was added to 50ml of the farmland recirculated water which is used without any purification. The resulting solution was used for preparation of the 0.05 M TBAB containing ethanol solution in volume ratio of 6:4.

## 3. RESULTS AND DISCUSSION

Figure 1 shows the SEM images of rGO/GCE, ZnS@$Ni_2P$/GCE and ZnS@$Ni_2P$/rGO/GCE. As seen from Figure 1a, the surface morphology of rGO reveals oriented 2D nanosheets as randomly aggregated and crumpled silk veil waves with ordered layer structure which are not perfectly flat. The nanosheets are rippled and entangled with each other because of the van der Waal's interactions between the sheet layers [34]. Figure 1 exhibits the morphology of the electrodeposited ZnS@$Ni_2P$ composite on GCE which indicates the deposition of typically sphere-shaped nanoparticles with a size of 70-100 nm. Figure 1c also shows the SEM image of electrodeposited ZnS@$Ni_2P$/rGO on GCE. As seen, the defects on rippled nanosheets of rGO provide a substrate for more porous electrodeposition

of ZnS@$Ni_2P$ nanoparticles which leads to a higher effective surface area and can effectively promote the electron transfer of the electrode [35, 36].

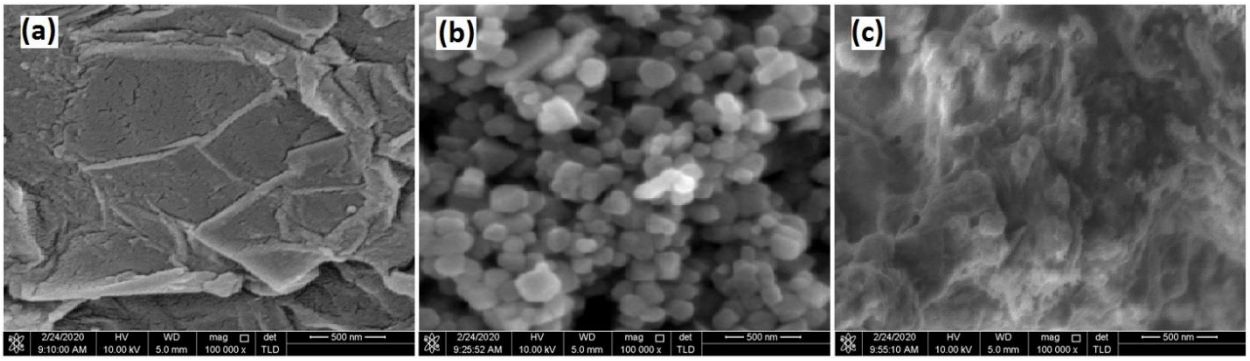


**Figure 1.** SEM images of (a) rGO/GCE, (b) ZnS@$Ni_2P$/GCE and (c) ZnS@$Ni_2P$/rGO/GCE.

Figure 2 shows the XRD patterns of powders of electrodeposited rGO, ZnS, $Ni_2P$, ZnS@$Ni_2P$ and ZnS@$Ni_2P$/rGO. As seen from Figure 1a, the diffraction pattern of rGO shows two peaks at 2θ = 26.25° and 43.64° which are indexed to (002) and (100) reflection planes, respectively, and correspond to the hexagonal graphite peak for the rGO nanosheets (JCPDS card No. 00-41-1487) [37]. Figure 2b depicts the diffraction peaks at 2θ = 27.09°, 28.91°, 30.88°, 48.07°, 57.13° and 60.69° which is attributed to the characteristic (100), (002), (101), (110), (112) and (201) planes of wurtzite ZnS, respectively (JCPDS card No. 00-05-0492). The XRD pattern of $Ni_2P$ in Figure 2c shows the diffraction peaks at 2θ = 40.54°, 44.65°, 47.47° and 54.14° which corresponded to the formation of (111), (201), (210) and (300) planes of hexagonal $Ni_2P$, respectively (JCPDS card No. 03-065-1989). The XRD patterns of ZnS@$Ni_2P$ and ZnS@$Ni_2P$/rGO in Figures 2d and 2e display the peaks of ZnS and $Ni_2P$, and ZnS@$Ni_2P$/rGO shows the additional peak of (100) plane of rGO. The results of SEM and XRD indicate high crystalline growth of nanostructures and successful simultaneous electrodeposition of ZnS and $Ni_2P$ nanoparticles in ZnS@$Ni_2P$ and ZnS@$Ni_2P$/rGO on GCE.

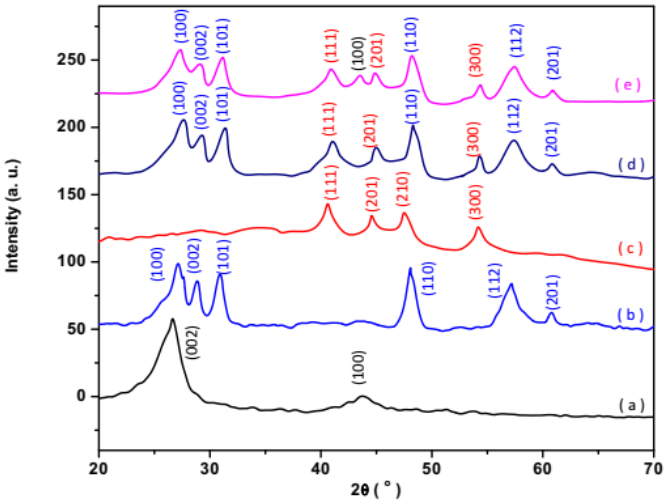


**Figure 2.** XRD pattern of electrodeposited (a) rGO, (b) ZnS, (c) $Ni_2P$, (d) ZnS@$Ni_2P$ and (e) ZnS@$Ni_2P$/rGO.

The electrochemical behavior of GCE, rGO/GCE, ZnS/GCE, $Ni_2P$/GCE, ZnS@$Ni_2P$/GCE and ZnS@$Ni_2P$/rGO/GCE were studied using DPV in 0.05 M TBAB containing ethanol solution and 3 µM CPS d in the potential range from -1.1 to 0.0 V at a scanning rate of 25 mV/s. Figure 3 exhibits the DPV curves of all electrodes, representing the of GCE does not show any anodic and cathodic peaks, and rGO/GCE, ZnS/GCE, Ni2P/GCE, ZnS@Ni2P/GCE and ZnS@Ni2P/rGO/GCE show an anodic peak at a potential of around -0.91V, that is associated with the electrochemical reduction of - C=N of the pyridine moiety in chlorpyrifos [38]. As shown, modification of the GCE using rGO in rGO/GCE and ZnS@$Ni_2P$/rGO/GCE significantly increased the electrocatalytic response of electrodes that it attributed to large surface area, interconnected macroporous structures, good conductivity and ultrahigh loading capacity for analytes [39, 40].2D rGO nanosheets provide defects and numerous edges as the active sites to reduce CPS [41]. The highest electrocatalytic response belongs to ZnS@$Ni_2P$/rGO/GCE that is related to the synergistic effects between ZnS@$Ni_2P$ and rGO which promoted the sensitivity of the electrode [42, 43]. The hollow structure of the rGO ananosheets and ZnS and $Ni_2P$ nanoparticles can supply more electrocatalytic active sites than rGO/GCE, ZnS/GCE, $Ni_2P$/GCE, ZnS@$Ni_2P$/GCE [44]. The ZnS@$Ni_2P$/rGO forms a good conductive network to enhance the conductivity and catalytic activity of the modified electrode [45]. The ability of ZnS and Ni2P to transmit and conduct charges is significantly improved after electrodepositin of nanoparticles on rGO, substitution of ZnS and phosphorus atoms [45, 46]. As a result, the following electrochemical experiments on ZnS@$Ni_2P$/rGO/GCE were carried out.

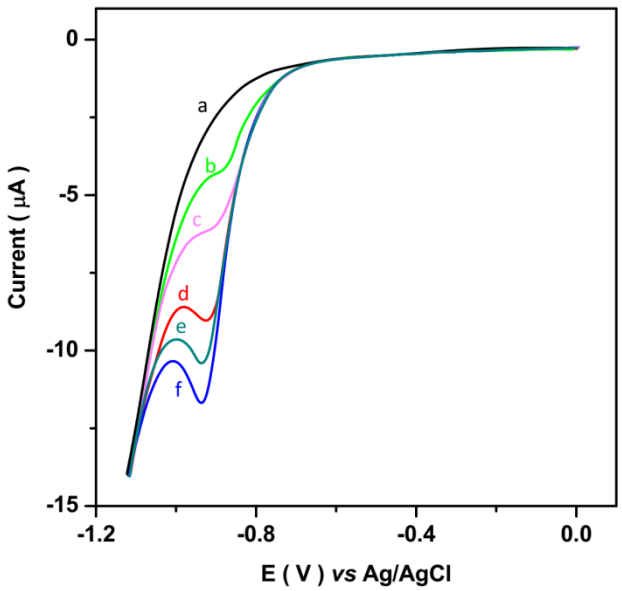


**Figure 3.** The DPV curves of (a) GCE, (b) rGO/GCE, (c) ZnS/GCE, (d) $Ni_2P$/GCE, (e) ZnS@$Ni_2P$/GCE and (f) ZnS@$Ni_2P$/rGO/GCE in 0.05 M TBAB containing ethanol solution and 3 µM CPS d in the potential range from -1.1 to 0.0 V at a scanning rate of 25 mV/s.

Figure 4 depicts the stability effect of the electrochemical response of ZnS@$Ni_2P$/rGO/GCE in 0.05 M TBAB containing ethanol solution and 3 µM CPS d in the potential range from -1.1 to 0.0 V at a scanning rate of 25 mV/s. As observed, the first and 100$^{th}$ DPV curves reveal a less than 3% decrease

in peak current in the presence of 3 µM CPS which is evidence of the great stability of ZnS@$Ni_2P$/rGO/GCE response for determination of CPS that can be related to the highly conducting porous architecture of rGO. In addition, ZnS and $Ni_2P$ nanoparticles are well assembled with rGO nanosheets in the electrodeposition process which can offer mechanical and chemical stability during continuous electrochemical analyses [45-47].

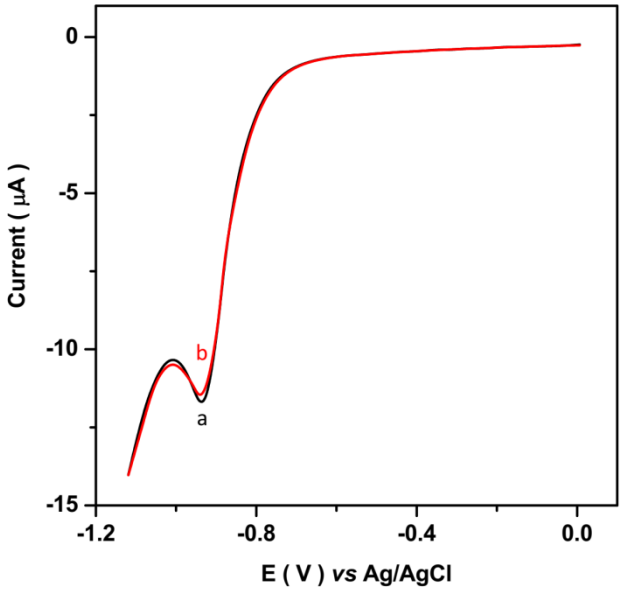


**Figure 4**. The (a) first and (b) 100$^{th}$ DPV curves of ZnS@$Ni_2P$/rGO/GCE in 0.05 M TBAB containing ethanol solution and 3 µM CPS in the potential range from -1.1 to 0.0V at a scanning rate of 25mV/s.

Figure 5 shows the amperometry response and resultant calibration plot of ZnS@$Ni_2P$/rGO/GCE in 0.05 M TBAB containing ethanol solution at a potential of -0.91V and 1000 rpm rotating speed under successive addition of 25µM CPS. As seen, there is a fast response of modified electrode after each addition of 100 µM CPS solution, and the amperometric current is linearly increased with increasing the CPS concentration. The results suggest obtaining a wide linear response range from 25 to 375 µM with a high sensitivity of 0.89799µA/µM and a limit of detection of 0.004 µM. The results of amperometry measurements of ZnS@$Ni_2P$/rGO/GCE are compared by the other reported CPS sensors in Table 1. It can be found that the sensor in this study shows comparable electrochemical performance to the previously reported sensors which is correlated to the high electron transfer rate contributed by the edge-rich architecture of the rGO and catalysis sites of ZnS and $Ni_2P$ nanoparticles [48, 49].

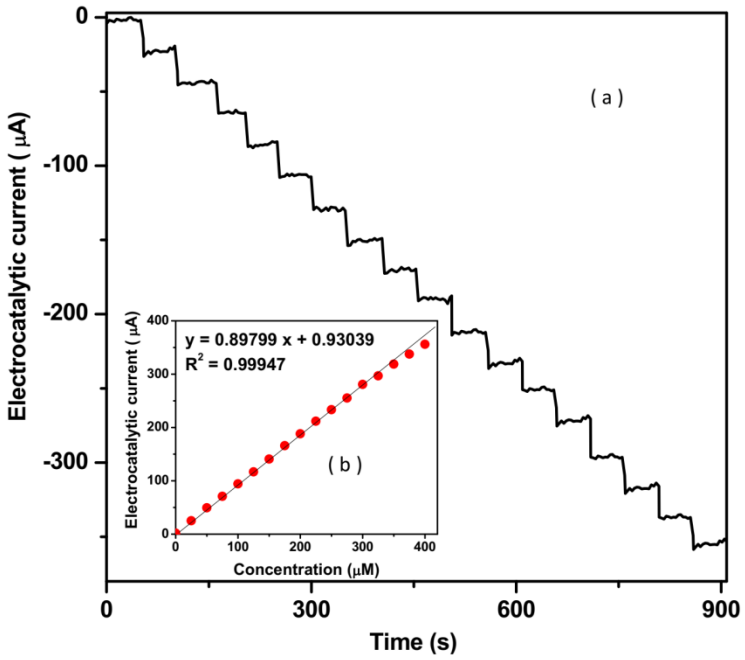


**Figure 5.** (a) The amperometry response and (b) resulted calibration plot of ZnS@$Ni_2P$/rGO/GCE in 0.05 M TBAB containing ethanol solution at potential of -0.91V and 1000 rpm rotating speed under successive addition of 25μM CPS.

**Table 1.** Comparison between the sensing properties of ZnS@$Ni_2P$/rGO/GCE and other reported CPS sensors.

| **Electrode** | **Technique** | **Linear Range (μM)** | **limit of detection (μM)** | **Ref.** |
|---|---|---|---|---|
| ZnS@$Ni_2P$/rGO/GCE | Amperometry | 25 to 375 | 0.004 | This work |
| $TiO_2$/cellulose acetate/GCE | Amperometry | 20 to 340 | 11.8 | [50] |
| $TiO_2$/cellulose acetate/GCE | CV | 10 to 130 | 4.4 | [50] |
| Ag nanoparticles/rGO-$NH_2$ | CV | 0.06 to 0.348 | 0.04 | [51] |
| poly 3, 4-ethylenedioxythiophene/GCE | CV | 0.001 to 0.7 | $8x10^{-4}$ | [52] |
| Hanging mercury drop electrode | DPCASV | 0.099 to 0.596 | 0.099 | [53] |
| Clay/carbon paste electrode | AdSV | $2.8x10^{-4}$ to 5.7 | $2.2x10^{-4}$ | [54] |
| Hanging mercury drop electrode | DPV | 0.057 to 0.285 | $4.0x10^{-4}$ | [55] |
| molecularly imprinted polymer/GCE | DPV | $10^{-4}$ to 100 | 0.004 | [56] |
| Dropping mercury electrode | DPP | 0.97 to 6.9 | 0.87 | [57] |

CV: cyclic voltammetry; DPCASV: differential pulse cathodic adsorptive stripping voltammetry; AdSV: adsorptive stripping voltammetry; DPP: Differential pulse polarography

Further electrochemical studies were carried out to investigate the selectivity and interference response of ZnS@$Ni_2P$/rGO/GCE for determination of CPS in presence of interferents. Table 2 shows the resultant electrocatalytic currents of ZnS@$Ni_2P$/rGO/GCE using amperometric measurements in 0.05 M TBAB containing ethanol solution at potential of -0.91V and 1000 rpm rotating speed under successive addition of 2µM of CPS solution and 8 µM of various inorganic ions and industrial pesticides in wastewater as possible interfering agents. Results show that the response of ZnS@$Ni_2P$/rGO/GCE toward addition of CPS is outstandingly great than that toward the addition of other species which implied the selective response of the proposed electrode as CPS sensor, and the species in Table 2 did not interfere with the amperometric determination of a CPS at potential of -0.91V.

**Table 2.** The resulted eletrocatalytic currents of ZnS@$Ni_2P$/rGO/GCE using amperometric measurements in 0.05 M TBAB containing ethanol solution at potential of -0.91V and 1000 rpm rotating speed under successive addition of 2µM of CPS solution and 8 µM of various interfering agents.

| specie | **Concentration (µM)** | **Amperometric current (µA) at -0.91V** | **RSD (%)** |
|---|---|---|---|
| CPS | 2 | 1.787 | ±0.098 |
| $Mg^{2+}$ | 8 | 0.212 | ±0.010 |
| $Ca^{2+}$ | 8 | 0.117 | ±0.009 |
| $NH_4$ | 8 | 0.318 | ±0.008 |
| $Na^+$ | 8 | 0.078 | ±0.007 |
| $K^+$ | 8 | 0.084 | ±0.008 |
| fenitrothion | 8 | 0.121 | ±0.011 |
| Dichlorvos | 8 | 0.132 | ±0.010 |
| Ethoprophos | 8 | 0.278 | ±0.017 |
| Disulfoton | 8 | 0.103 | ±0.007 |
| Parathion-methyl | 8 | 0.105 | ±0.004 |
| Fenchlorphos | 8 | 0.092 | ±0.008 |
| Prothiofos | 8 | 0.077 | ±0.004 |
| Azinphos-methyl | 8 | 0.107 | ±0.007 |
| Malathion | 8 | 0.241 | ±0.009 |

RSD: relative standard deviation

For investigation into the applicability of the modified CPS sensors in prepared real sample of farmland recirculated water, the amperomery experiments were performed using ZnS@$Ni_2P$/rGO/GCE in a prepared real sample of farmland recirculated water with 0.05 M TBAB containing ethanol solution at a potential of -0.91V and 1000 rpm rotating speed under successive addition of 1µM of CPS solutions. Figure 6 displays the amperometry response and resulting calibration plot which indicted to good linearity. The CPS concentration in a prepared real sample of farmland recirculated water is estimated at 0.016 µM which is very close to initial concentration of injected CPS solution in preparation process of the real sample. Furthermore, the accuracy of the ZnS@$Ni_2P$/rGO/GCE was

investigated using a conventional addition approach to evaluate CPS in prepared actual samples. Table 3 shows the satisfactory precision with acceptable recovery (≥ 92.50%) and RSD (≤3.31%) values. Therefore, ZnS@$Ni_2P$/rGO/GCE can be reliably determined CPS in farmland recirculated water and agricultural wastewater specimens.

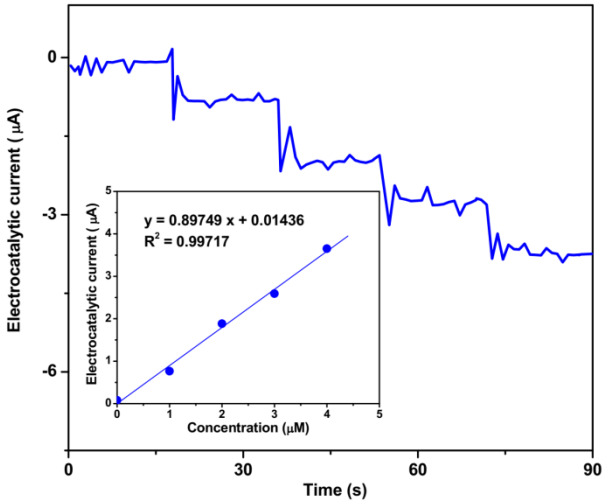


**Figure 6.** (a) The amperometry response and (b) resulted calibration plot of ZnS@$Ni_2P$/rGO/GCE in 0.05 M TBAB containing ethanol solution at potential of -0.91V and 1000 rpm rotating speed under successive addition of 1μM CPS.

**Table 3.** Analytical results of ZnS@$Ni_2P$/rGO/GCE to determine CPS in prepared real samples of farmland recirculated water.

| **Added(mg/ml)** | **Found(mg/ml)** | **Recovery (%)** | **RSD (%)** |
|---|---|---|---|
| 1.00 | 0.97 | 97.00 | 2.21 |
| 2.00 | 1.85 | 92.50 | 2.84 |
| 3.00 | 2.78 | 92.66 | 3.31 |
| 4.00 | 3.89 | 97.25 | 3.23 |

## 4. CONCULUSION

This study was carried out to synthesis ZnS@$Ni_2P$/rGO/GCE as an electrochemical sensor of CPS in farmland recirculated waters. rGO, ZnS and $Ni_2P$ nanoparticles were electrodeposited on the GCE surface. Results of morphological and structural analyses revealed the successful simultaneous electrodeposition of ZnS and $Ni_2P$ nanoparticles in ZnS@$Ni_2P$ and ZnS@$Ni_2P$/rGO on GCE. Results of electrochemical studies indicated sensitive, selective and stable responses of ZnS@$Ni_2P$/rGO/GCE to presence of CPS. Results implied obtaining a wide linear response range from 25 to 375 μM with a high sensitivity of 0.89799μA/μM and a limit of detection of 0.004 μM. The results of the study on the applicability of modified CPS sensors in prepared real sample of farmland recirculated water showed

the satisfactory precision with acceptable recovery and RSD values. Thus, ZnS@$Ni_2P$/rGO/GCE can be reliably determined the CPS in farmland recirculated water and agricultural wastewater samples.

ACKNOWLEDGEMENT
Process and mechanism of nitrogen transfer and transformation in Xueye Lake Basin Based on Distributed Hydrological Model (2021qnzx02).

## References

1. R.A. Hites, *Environmental Science & Technology*, 55 (2021) 1354.
2. W.-Y. Huang, G.-Q. Wang, W.-H. Li, T.-T. Li, G.-J. Ji, S.-C. Ren, M. Jiang, L. Yan, H.-T. Tang and Y.-M. Pan, *Chem*, 6 (2020) 2300.
3. S.Y. Foong, N.L. Ma, S.S. Lam, W. Peng, F. Low, B.H. Lee, A.K. Alstrup and C. Sonne, *Journal of hazardous materials*, 400 (2020) 123006.
4. Y. Duan, Y. Liu, Z. Chen, D. Liu, E. Yu, X. Zhang, H. Fu, J. Fu, J. Zhang and H. Du, *Green Chemistry*, 22 (2020) 44.
5. D.S. Dos Santos, M.E. Rosa, A.P. Zanatta, R.S. Oliveira, C.G.M. de Almeida, A.P. Leal, M. Sanz, K.A. Fernandes, V.Q. de Souza and D.R. de Assis, *Ecotoxicology and environmental safety*, 171 (2019) 138.
6. S. Ren, B. Ye, S. Li, L. Pang, Y. Pan and H. Tang, *Nano Research*, (2021) 1.
7. Y. Orooji, B. Tanhaei, A. Ayati, S.H. Tabrizi, M. Alizadeh, F.F. Bamoharram, F. Karimi, S. Salmanpour, J. Rouhi and S. Afshar, *Chemosphere*, 281 (2021) 130795.
8. M. Pirsaheb, N. Fattahi, R. Rahimi, K. Sharafi and H.R. Ghaffari, *Food chemistry*, 231 (2017) 148.
9. R. Wang, Y. Yuan, J. Zhang, X. Zhong, J. Liu, Y. Xie, S. Zhong and Z. Xu, *Journal of Power Sources*, 501 (2021) 230006.
10. A. Kushwaha, G. Singh and M. Sharma, *RSC Advances*, 10 (2020) 13050.
11. K. Zhang, L. Qiu, J. Tao, X. Zhong, Z. Lin, R. Wang and Z. Liu, *Hydrometallurgy*, 205 (2021) 105722.
12. R. Miao, J. Ma, Y. Liu, Y. Liu, Z. Yang and M. Guo, *Forests*, 10 (2019) 188.
13. R.D. Burke, S.W. Todd, E. Lumsden, R.J. Mullins, J. Mamczarz, W.P. Fawcett, R.P. Gullapalli, W.R. Randall, E.F. Pereira and E.X. Albuquerque, *Journal of neurochemistry*, 142 (2017) 162.
14. Z. Fan, P.-p. Ji, J. Zhang, D. Segets, D.-R. Chen and S.-C. Chen, *Journal of Membrane Science*, 635 (2021) 119503.
15. X. Zhang, Y. Tang, F. Zhang and C.S. Lee, *Advanced Energy Materials*, 6 (2016) 1502588.
16. S. Armenta, G. Quintás, S. Garrigues and M. de la Guardia, *Talanta*, 67 (2005) 634.
17. O. Zalat, M. Elsayed, M. Fayed and M. Abd El Megid, *International Letters of Chemistry, Physics and Astronomy*, 2 (2014) 58.
18. P. Wang, M. Rashid, J. Liu, M. Hu and G. Zhong, *Food chemistry*, 212 (2016) 420.
19. Y. Lee, Y.J. Kim, M.S.I. Khan and Y.C. Na, *Journal of Separation Science*, 43 (2020) 4047.
20. S.N. Sinha, R. Pal, A. Dewan, M. Mansuri and H. Saiyed, *International Journal of Mass Spectrometry*, 253 (2006) 48.
21. Z. Song, S. Hou and N. Zhang, *Journal of agricultural and food chemistry*, 50 (2002) 4468.
22. J. Xiong, X. Tang, G. Zhou, Z. Guan and L. Wu, *Analytical Methods*, 5 (2013) 536.
23. M.A. Martínez, S. Ballesteros, C. Sánchez de la Torre, A. Sanchiz, E. Almarza and A. García-Aguilera, *Journal of analytical toxicology*, 28 (2004) 609.

24. D. Chen, Y. Jiao, H. Jia, Y. Guo, X. Sun, X. Wang and J. Xu, *International Journal of Electrochemical Science*, 10 (2015) 10491.
25. H. Wang, G. Zhao, D. Chen, Z. Wang and G. Liu, *International Journal of Electrochemical Science*, 11 (2016) 10906.
26. I.B. Salem, M. Errami, M. Mezni, R. Salghi, E.E. Ebenso, B. Hammouti, S. Fattouch and F. Rabouti, *International Journal of Electrochemical Science*, 9 (2014) 342.
27. S. Li, R. Liang, W. Qin, R. Yao and R. Liang, *International Journal of Electrochemical Science*, 10 (2015) 1393 -.
28. H. Karimi-Maleh, Y. Orooji, F. Karimi, M. Alizadeh, M. Baghayeri, J. Rouhi, S. Tajik, H. Beitollahi, S. Agarwal and V.K. Gupta, *Biosensors and Bioelectronics*, 184 (2021) 113252.
29. R. Wang, H. Xie, X. Lai, J.-B. Liu, J. Li and G. Qiu, *Molecular Catalysis*, 515 (2021) 111881.
30. L. Chen, Y. Tang, K. Wang, C. Liu and S. Luo, *Electrochemistry communications*, 13 (2011) 133.
31. K. Ghezali, L. Mentar, B. Boudine and A. Azizi, *Journal of Electroanalytical Chemistry*, 794 (2017) 212.
32. A. Kassim, S. Nagalingam, H.S. Min and N. Karrim, *Arabian Journal of Chemistry*, 3 (2010) 243.
33. V.T. Chebrolu, B. Balakrishnan, S.A. Raja, I. Cho, J.-S. Bak and H.-J. Kim, *New Journal of Chemistry*, 44 (2020) 7690.
34. X. Fan, Y. Hu, Y. Zhang, J. Lu, X. Chen, J. Niu, N. Li and D. Chen, *Coatings*, 9 (2019) 666.
35. C. Xiong, B. Li, X. Lin, H. Liu, Y. Xu, J. Mao, C. Duan, T. Li and Y. Ni, *Composites Part B: Engineering*, 165 (2019) 10.
36. H. Guan, S. Huang, J. Ding, F. Tian, Q. Xu and J. Zhao, *Acta Materialia*, 187 (2020) 122.
37. N. Zhao, L. Deng, D. Luo and P. Zhang, *Applied Surface Science*, 526 (2020) 146696.
38. J. Fischer, A. Hájková, M. Pereira, M. Křeček, V. Vyskočil and J. Barek, *Electrochimica Acta*, 216 (2016) 510.
39. D. Chanda, J. Hnát, A.S. Dobrota, I.A. Pašti, M. Paidar and K. Bouzek, *Physical Chemistry Chemical Physics*, 17 (2015) 26864.
40. H. Cheng, T. Li, X. Li, J. Feng, T. Tang and D. Qin, *Journal of The Electrochemical Society*, 168 (2021) 087504.
41. T. Tite, E.A. Chiticaru, J.S. Burns and M. Ioniţă, *Journal of nanobiotechnology*, 17 (2019) 1.
42. S. Liu, L. Ma, H. Zhang and C. Ma, *Materials Research Bulletin*, 77 (2016) 271.
43. S.A. Alkahtani, A.M. Mahmoud, M.H. Mahnashi, A.O. AlQarni, Y.S. Alqahtani and M.M. El-Wekil, *Microchemical Journal*, 164 (2021) 105972.
44. P. Zhang, C. Xue, Y. Li, S. Guo, X. Zhang, P. Zhang and G. Shao, *Chemical Engineering Journal*, 404 (2021) 126497.
45. S. Luo, R. Wang, P. Hei, L. Gao, J. Yang and T. Jiao, *Colloids and Surfaces A: Physicochemical and Engineering Aspects*, 612 (2021) 125992.
46. Z. Lv, Q. Zhong and Y. Bu, *Applied Surface Science*, 439 (2018) 413.
47. Z. Jiang, J. Yu, X. Song, W. Yang, H. Fang, Y. Sun, G. Sun and T. Huang, *New Journal of Chemistry*, 42 (2018) 19285.
48. V.V. Tran, D.D. Nguyen, M. Hofmann, Y.-P. Hsieh, H.-C. Kan and C.-C. Hsu, *Nanomaterials*, 11 (2021) 511.
49. X. Zhang, X. Sun, T. Lv, L. Weng, M. Chi, J. Shi and S. Zhang, *Journal of Materials Science: Materials in Electronics*, 31 (2020) 13344.
50. A. Kumaravel and M. Chandrasekaran, *Journal of agricultural and food chemistry*, 63 (2015) 6150.
51. M. Guler, V. Turkoglu and Z. Basi, *Electrochimica Acta*, 240 (2017) 129.
52. P. Manisankar, S. Viswanathan, A.M. Pusphalatha and C. Rani, *Analytica Chimica Acta*, 528 (2005) 157.

53. M. El-Shahawi and M. Kamal, *Fresenius' journal of analytical chemistry*, 362 (1998) 344.
54. K. Sirisha, S. Mallipattu and S.R. Jayarama Reddy, *Analytical letters*, 40 (2007) 1939.
55. F.O. Pelit, H. Ertaş and F.N. Ertaş, *Journal of Applied Electrochemistry*, 41 (2011) 1279.
56. W. Xu, Q. Wang, W. Huang and W. Yang, *Journal of separation science*, 40 (2017) 4839.
57. A. Al-Meqbali, M. El-Shahawi and M. Kamal, *Electroanalysis: An International Journal Devoted to Fundamental and Practical Aspects of Electroanalysis*, 10 (1998) 784.